Enhanced Chaos Game Optimization for Multilevel Image Thresholding through Fitness Distance Balance Mechanism

Achraf Ben Miled
Computer Science Department, Science College, Northern Border University, Saudi Arabia
ashraf.benmilad@nbu.edu.sa (corresponding author)

Mohammed Ahmed Elhossiny
Applied College, Northern Border University, Saudi Arabia | Faculty of Specific Education, Mansoura University, Egypt
mohammed.elhossiny@nbu.edu.sa

Marwa Anwar Ibrahim Elghazawy
Applied College, Northern Border University, Saudi Arabia
miss_marwa80@hotmail.com

Ashraf F. A. Mahmoud
Computer Science Department, Science College, Northern Border University, Saudi Arabia
ashraf.abubaker@nbu.edu.sa

Faroug A. Abdalla
Computer Science Department, Science College, Northern Border University, Saudi Arabia
faroug.abdalla@nbu.edu.sa

Received: 2 May 2024 | Revised: 13 May 2024 | Accepted: 15 May 2024

 DOI: https://doi.org/10.48084/etasr.7713

ABSTRACT

This study proposes a method to enhance the Chaos Game Optimization (CGO) algorithm for efficient multilevel image thresholding by incorporating a fitness distance balance mechanism. Multilevel thresholding is essential for detailed image segmentation in digital image processing, particularly in environments with complex image characteristics. This improved CGO algorithm adopts a hybrid metaheuristic framework that effectively addresses the challenges of premature convergence and the exploration-exploitation balance, typical of traditional thresholding methods. By integrating mechanisms that balance fitness and spatial diversity, the proposed algorithm achieves improved segmentation accuracy and computational efficiency. This approach was validated through extensive experiments on benchmark datasets, comparing favorably against existing state-of-the-art methods.

Keywords-chaos game optimization; fitness distance balance; multilevel image thresholding; computer vision; optimization algorithms

I. INTRODUCTION

Image segmentation is a fundamental problem in digital image analysis involving partitioning images into semantically uniform regions or objects. Among existing segmentation techniques, thresholding aims to separate foreground from background pixels based on intensity value differences using one or more threshold values [1]. However, selecting optimal thresholds remains challenging due to intrinsic image complexities and application-dependent variability in factors, such as illumination, contrast, noise, and scene content. Traditional thresholding methods often need more robustness to adapt to heterogeneity in real-world settings. Global thresholding techniques, like the Otsu method, are simple but sensitive to noise and intensity inhomogeneity [2]. Local thresholding somewhat addresses this issue but requires additional parameters and computational effort. Furthermore, existing techniques primarily focus on bi-level thresholding,

whereas many applications demand multi-thresholding to partition multi-modal intensity distributions.

Metaheuristic optimization algorithms have proven effective for large and complex search spaces by iteratively exploring and exploiting the solution landscape according to heuristic principles [3-4]. This makes them well-suited to enhance thresholding techniques by formulating selection as an optimization task to determine thresholds that maximize segmentation performance, image quality, and accuracy criteria. Previous studies incorporated metaheuristics, namely Genetic Algorithms (GAs), Particle Swarm Optimization (PSO), and ant colony optimization, into thresholding, demonstrating improved adaptability and effectiveness compared to traditional methods. However, existing approaches also encounter limitations from premature convergence, local optima trapping, and computational inefficiency, particularly for multi-modal images that require multi-thresholding [5]. Moreover, different applications demand specialized thresholding capabilities that are suited to their characteristic data and constraints. Therefore, more innovation is needed to develop hybrid metaheuristic frameworks that synthesize the complementary strengths of multiple algorithms for enhanced adaptability, robustness, and computational efficiency in diverse contexts.

This study aims to significantly improve the efficiency and accuracy of the Chaos Game Optimization (CGO) algorithm for multilevel image thresholding. This study introduces a novel Fitness Distance Balance (FDB) mechanism that combines metaheuristic optimization with principles of chaos theory to address premature convergence and enhance the exploration-exploitation balance. This mechanism allows the algorithm to dynamically adjust search strategies based on real-time performance metrics, thus improving segmentation results in complex imaging environments. Validated through comprehensive experiments on benchmark datasets, this approach not only surpasses traditional methods but also highlights the potential of hybrid metaheuristic strategies in advanced image processing applications.

II. META-HEURISTIC OPTIMIZATION IN MULTILEVEL THRESHOLD IMAGE SEGMENTATION

Metaheuristic algorithms have been pivotal in exploring image segmentation techniques, particularly multilevel thresholding. The Artificial Bee Colony (ABC) algorithm stands out for its innovative applications and adaptations, significantly enhancing the field's capabilities. The MEABCT algorithm [6] represents a paradigm shift by offering substantial improvements in segmentation accuracy over established methods, such as honey bee mating optimization, hybrid cooperative comprehensive learning-based algorithms, the Otsu method, and PSO. This algorithm has demonstrated exceptional proficiency in identifying thresholds that closely align with the optimal one, showcasing its suitability for complex segmentation tasks. The Modified ABC (MABC) algorithm [7] enhanced image segmentation by integrating opposition-based learning and chaotic systems, outperforming traditional techniques involving genetic and PSO in precision. The KABC algorithm [8] merged ABC with the krill herd algorithm and leveraged the HSV color scale and structural similarity index matrix to successfully deal with luminance variations, improving segmentation accuracy. A novel three-stage process synergized ABC with particle swarm and ant colony optimization algorithms [9], demonstrating its effectiveness over conventional methods through rigorous statistical validation, and showcasing the potential of metaheuristic strategies to advance image segmentation.

Parallel to the development of ABC-based methods, the Bacterial Foraging Algorithm (BFA) was adapted and refined for multilevel thresholding challenges. A variant of this approach, the modified BFA, demonstrated its ability to identify optimal thresholds through comparisons with PSO, standard BFA, and GAs [10]. In addition, cooperative BFA [11] and hybrid approaches incorporating bat algorithms [12] have contributed to the evolution of segmentation methods, each offering unique solutions to optimize threshold values for enhanced image segmentation. The Cuckoo Search Algorithm (CSA) has also seen significant application in this field, with variants, such as wind-driven optimization coupled with CSA [13] and adaptive CSA [14] being developed to optimize multilevel thresholding. These CSA-based methods have demonstrated their efficacy in achieving accurate and efficient segmentation results across various applications, from satellite image segmentation to coastal video image analysis.

In [15], the Electromagnetic Optimization (EMO) algorithm was introduced, enhanced by a multilevel thresholding approach and the Levy function, termed EMO-Levy. This algorithm stands out for its ability to determine optimal threshold values with a reduced number of iterations, showing superior efficiency and effectiveness relative to existing methods. Further innovation was introduced by the Chaotic Electromagnetic Field Optimization (CEFO) algorithm, which amalgamated the Electromagnetic Field Optimization (EFO) technique with fuzzy entropy criteria and a novel chaotic strategy. This approach outperformed other well-established algorithms in multilevel thresholding for color image segmentation, underscoring its superior performance and potential to incorporate chaotic dynamics into EMO strategies [16].

Various studies have introduced novel approaches to multilevel thresholding optimization putting into service PSO and its variants. For instance, a collaborative learning-based PSO variant, termed HCO-CLPSO, demonstrated enhanced performance by breaking down high-dimensional swarms into one-dimensional and employing complete learning approaches [17]. Additionally, integrating PSO with quantum principles, as seen in QPSO and CQPSO, improves segmentation accuracy and computational efficiency [18, 19]. Other approaches, such as DMTBPSO [20] and IPSO [21], deployed dynamic threshold filtering and chaotic sequences to improve PSO's searching ability, resulting in superior segmentation outcomes. Hybrid methods, like KPSO [22], which combines K-means, PSO, and learning automata, and Fibonacci PSO (FPSO) [23] achieved competitive segmentation results. Moreover, PSO variations entailing HCPSO [24] and NrQPSO [25] addressed issues such as premature convergence and computation efficiency, exhibiting notable advancements in image segmentation. Furthermore, specialized adaptations, namely

APSOW [26] for color image thresholding, demonstrated significant improvements in segmentation accuracy and robustness. These studies demonstrate the continuous evolution of PSO-based approaches and their competence in optimizing multilevel thresholding for image segmentation.

GAs have been widely used for multilevel image thresholding due to their ability to efficiently search large and complex solution spaces. In [27], wavelet transform was employed to first shorten the length and complexity of an image histogram, before applying a GA to determine the optimal number of thresholds and their values in the reduced histogram, and then project the thresholds back to the original space. Similarly, combining the discrete wavelet transform with GA has been shown to improve the speed and accuracy of multilevel thresholding by first shortening the histogram before GA calculates thresholds and numbers on the reduced histogram for projection back to the original space [28]. Hybridizing GAs with other metaheuristics, such as PSO, can further optimize thresholding, as demonstrated in [29], which combined PSO and GA to address PSO's weakness of premature convergence, finding that the hybrid PSO-GA approach outperformed standard PSO. Spatial information inclusion can also ameliorate GA-based thresholding, as observed in [30], which considered the spatial context of an image by using an "energy curve" instead of a histogram as GA input, where comparative evaluations manifested that it was effective for context-sensitive segmentation. Meanwhile, quantum GAs have been applied to multilevel thresholding problems, such as IQGA [31], which incorporates adaptive rotation and cooperative learning to improve convergence, stability, and searchability over high-dimensional spaces, outperforming QGA, GA, and PSO in experiments. Therefore, the ability of GAs to efficiently explore large search spaces, combined with techniques, namely wavelet transforms [27-28], cooperative evolution [29], or spatial data inclusion [30], have supported their popularity for automatic multilevel image thresholding and segmentation applications.

Many innovative approaches have been introduced for multilevel thresholding in image segmentation, showcasing the effectiveness of various metaheuristic algorithms. In [32], the Galaxy-based Search Algorithm (GbSA) was presented as a metaheuristic approach for evolutionary algorithms, utilizing spiral arms and chaos enforced by the logistic map to efficiently locate optimal thresholds. In [33], a new swarm intelligence method was introduced for image segmentation, optimizing the Kapur and Tsallis objective functions and demonstrating reliability and effectiveness compared to traditional methods such as PSO. Hybrid Memetic Algorithms (MAs) were proposed in [34] to enhance standard evolutionary methods like as GAs, demonstrating improved segmentation accuracy and convergence speed compared to GA. In [35], the Chaotic Multi-Verse Optimizer (CMVO) method was proposed to effectively determine optimal thresholds using the Kapur objective function with substantial efficiency gains. In [36], a Grey Wolf Optimizer (GWO)-based approach was presented for multilevel thresholding, delivering robust and superior segmentation results compared to existing methods. In [37], the effectiveness of PSO and CSO was evaluated for multilevel thresholding, with displaying superior performance. In [38], the Masi-Water Cycle Algorithm (WCA) was introduced for color image segmentation, outperforming existing methods in terms of efficiency and accuracy.

In [39], an adaptive Genetic Optimization Algorithm (GOA) was suggested to optimize the multilevel Tsallis cross-entropy, demonstrating enhanced segmentation accuracy and efficiency compared to traditional methods. In [40], the Hybrid Harmony Search Optimization with Differential Evolution (HHO-DE) method was introduced, exhibiting essential improvements in segmentation effectiveness and efficiency compared to other techniques. In [41], segmentation by Salp Swarm Algorithm (SSA) was recommended, providing realistic segmentation effectiveness through levy flow enhancement, while in [42] a BMO-DE-based hybrid optimization method was introduced for effective image segmentation, surpassing the performance of existing methods. In [43], a Threshold Estimation Optimization (TEO) method was proposed, enhanced by Levy flying and exhibiting superior efficiency compared to conventional techniques. In [44], the Enhanced Moth flame Optimization Algorithm (EMA) was introduced for image segmentation, demonstrating high accuracy and reliability. The Logistic Chaotic Barnacles Mating Optimizer (LCBMO) method [45] effectively addressed multilevel threshold image segmentation challenges, offering optimal outcomes. In [46], the Volleyball Premier League with Whale Optimization Algorithm (VPLWOA) was proposed for multilevel image segmentation, outperforming existing methods in terms of efficiency and accuracy. In [47], a Modified Water Wave Optimization (MWWO) algorithm demonstrated efficient multilevel image segmentation with improved reliability and effectiveness compared to other techniques. In [48], a Black Widow Optimization (BWO)-based method was introduced to determine optimal thresholds, showing superior efficiency and reliability compared to other methods. In [49], the Opposition-Based Laplacian Equilibrium Optimizer (OB-L-EO) method was presented, exhibiting enhanced segmentation performance through improved search precision and convergence. In [50], the Modified Ant Lion Optimizer (MALO) technique was proposed for optimal threshold determination, demonstrating superior performance compared to traditional methods. Finally, in [51], the Marine Predators Algorithm (MPA) recommended, displaying its effectiveness in multilevel thresholding and establishing its reliability and efficiency in image segmentation tasks.

III. MULTILEVEL THRESHOLDING TECHNIQUES

Multilevel thresholding is an advanced image segmentation technique used to separate an image into multiple regions beyond the simple foreground and background classification offered by bi-level thresholding. This approach is particularly effective in complex imaging scenarios where multiple objects or features need to be distinguished. The efficacy of multilevel thresholding is based on the selection of optimal threshold values, which are determined through the maximization or minimization of a specific objective function. Among the various thresholding methods, Kapur's entropy and Otsu's between-class variance are the most prevalent. These techniques provide a systematic approach to determining the thresholds that best segment an image.

A. Kapur's Entropy Method

Kapur's entropy method [52] is based on the concept of entropy maximization to determine the optimal thresholds that segment an image into multiple classes. In this context, the entropy of an image measures the information content that is essential for describing the complexity within it. The aim is to maximize the entropy across the classes formed by the thresholds, which corresponds to maximizing the information captured about the different regions. The method begins by calculating the probability of occurrence for each grayscale level in the image. This probability, denoted as p_i, is computed as the frequency of each level divided by the total number of pixels given by:

$$p_i = \frac{\eta_i}{N} \quad (1)$$

where η_i is the number of times a grayscale level i occurs, and N is the total number of pixels. For a set of thresholds $T = \{t_1, t_2, \dots, t_k\}$, the entropy for each segment is calculated. The total entropy $H(T)$ for these thresholds is the sum of the entropies of all segments:

$$H(T) = -\sum_{j=0}^{k} \sum_{i=t_j}^{t_{j+1}-1} p_i \, log(p_i) \quad (2)$$

where $t_0 = 0$ and $t_{k+1} = L$, with L being the maximum grayscale level. The optimal thresholds are those that maximize this total entropy.

B. Otsu's Between-Class Variance Method

The Otsu method [53], on the other hand, focuses on maximizing the between-class variance, thus enhancing the separability of classes. This method calculates the optimal threshold to minimize the intra-class variance or equivalently maximize the inter-class variance, which is a measure of how distinct the classes are. The initial step involves calculating the same probabilities p_i as in Kapur's method. Using these probabilities, the algorithm then calculates the total mean level of the image and the mean levels for each class defined by the thresholds. The between-class variance $\sigma_B^2(T)$ is defined by:

$$\sigma_B^2(T) = \sum_{j=0}^{k} \omega_i \left(\mu_j - \mu_T\right)^2 \quad (3)$$

where ω_i and μ_j are the probability and mean level of class j, respectively, and μ_T is the total mean level of the image. The thresholds that maximize this between-class variance are considered optimal, as they provide the clearest separation between classes.

Both Kapur's entropy and Otsu's between-class variance methods offer robust frameworks for determining the thresholds in multilevel thresholding. While the Kapur method maximizes the information content across the segmented regions, the Otsu method enhances class separability by maximizing the variance between them. The choice of method depends on the specific requirements of the image processing task and the characteristics of the image being analyzed. These techniques enable the effective segmentation of complex images into multiple meaningful regions, facilitating advanced image analysis tasks.

IV. PROPOSED APPROACH

The CGO algorithm [54] is constructed upon the theoretical foundations of the chaos theory, particularly emphasizing the principles of fractals and their application through the chaos game mechanism. This section delineates the mathematical formalization employed in CGO, which facilitates an innovative approach to optimization by incorporating the complex patterns and self-similarity inherent in fractals.

A. Chaos Game Optimization (CGO) Algorithm Formulation

The CGO algorithm integrates principles from the chaos theory and fractals, specifically using the Sierpinski triangle to shape the search space. It takes advantage of the structured, yet unpredictable nature of chaos games to effectively navigate through the solution space.

1) Initialization of Solution Candidates

The CGO algorithm starts with a set of solution candidates, denoted as X, which represent potential solutions within a Sierpinski triangle. Each solution candidate X_i consists of decision variables $x_{i,j}$, which position these candidates within the fractal search space. The mathematical representation of these candidates is given by:

$$X = \begin{bmatrix} x_{1,1} & x_{1,2} & \cdots & x_{1,d} \\ X_{2,1} & x_{2,2} & & x_{2,d} \\ \vdots & & \ddots & \vdots \\ x_{n,1} & x_{n,2} & \cdots & x_{n,d} \end{bmatrix}, \; i = 1, 2, \dots n \quad (4)$$

where n represents the number of solution candidates, and d is the dimensionality of the decision variables.

2) Initialization of Positions

The initial positions of these solution candidates, or seeds, are randomly determined within the predefined bounds of the search space:

$$x_{i,j}(0) = x_{i,j}^{min} + rand * \left(x_{i,j}^{max} - x_{i,j}^{min}\right), \quad i = 1, 2, \dots, n; \quad j = 1, 2, \dots, d \quad (5)$$

This initialization is crucial as it sets the starting points for the exploration of the search space.

3) Generation of New Candidates via Temporary Triangles

The core mechanism for generating new solution candidates involves the creation of temporary triangles utilizing three specific points:

- The position of the Global Best (GB),
- The position of the Mean Group (MG_i),
- The position of the selected solution candidate (X_i).

These points serve as vertices for temporary triangles within which new seeds are generated, simulating the iterative fractal construction of a Sierpinski triangle.

4) Mathematical Descriptions for Seed Updates

The equations describing the updates for seeds within these triangles are:

$$Seed1 = X_i + \alpha_i(\beta_i * GB - \gamma_i * MG_i) \quad (6)$$

$$Seed2 = GB + \alpha_i(\beta_i * X_i - \gamma_i * MG_i) \quad (7)$$

$$Seed3 = MG_i + \alpha_i(\beta_i * X_i - \gamma_i * GB) \quad (8)$$

$$i = 1, 2, \dots, n$$

These updates leverage chaos game dynamics to drive the exploration and exploitation processes, ensuring diverse and comprehensive search behavior.

5) Mutation and Exploration Control

The algorithm also includes a mutation mechanism to escape local optima:

$$Seed4 = X_i(x_k = x_k + R),\ k = [1, 2, \dots, d] \quad (9)$$

where R is a random number in the range [0, 1], and x_k is the k^{th} decision variable of the seed X_i. The exploration and exploitation rates are controlled by adjusting α_i, which modulates the influence radius around the seeds:

$$\alpha_i = \begin{cases} Rand \\ 2 * Rand \\ (\delta * Rand) + 1 \\ (\epsilon * Rand) + (\sim\epsilon) \end{cases} \quad (10)$$

The process iteratively evaluates the fitness of new seeds against existing ones, promoting only those that enhance the quality of the solution. This selection process is crucial to maintaining the integrity and effectiveness of the search strategy.

B. Fitness Distance Balance (FDB)

The FDB selection method [55] introduces a sophisticated approach designed to prevent premature convergence in meta-heuristic search algorithms. This method enhances the selection process by balancing the fitness and the diversity of candidates within the population, which is essential for effective exploration and exploitation. The calculation of the distance from each candidate to the best solution found so far is a critical first step. This distance is calculated using the Euclidean formula:

$$D_i = \sqrt{\sum_{j=1}^{d} \left(x_{i,j} - x_{best\,j}\right)^2} \quad (11)$$

where D_i denotes the distance of the i^{th} candidate from the best solution, $x_{i,j}$ represents the j^{th} dimension of the i^{th} candidate, $x_{best\,j}$ is the j^{th} dimension of the best solution found, and d is the total number of dimensions in the problem space.

Following the computation of distances, both the fitness values and the distances are normalized to prevent any single metric from dominating the selection process. Normalization ensures a balanced consideration of both fitness and diversity, supporting a more robust global search capability by maintaining genetic diversity within the population. The score for each candidate is then calculated using a weighted sum of the normalized fitness and normalized distance, which facilitates the selection of candidates that are not only promising in terms of their fitness, but also diverse enough from the best solution to explore potentially unsearched areas of the solution space:

$$Score_i = \omega * normFitness_i + (1 - \omega) * normDistance_i \quad (12)$$

where ω is a weight factor between 0 and 1 that balances the influence of fitness and distance on the score. Adjusting ω allows the algorithm to emphasize exploration or exploitation as needed by the specific dynamics of the search process or stages of algorithm convergence. This method has been validated through extensive empirical testing across various benchmark functions, demonstrating its ability to enhance the search performance of meta-heuristic algorithms by preventing premature convergence and maintaining a diverse set of solutions.

C. FDB-CGO Algorithm

The primary objective of modifying the exploration strategy within the CGO algorithm is to transition from a purely random seed generation to a more guided and adaptive approach [56]. This modification intends to augment the CGO's exploration capabilities by strategically leveraging insights accrued throughout the optimization process. The refined strategy not only enhances the algorithm's potential to escape local optima, but also aims to efficiently exploit promising regions of the search space, thus expediting convergence towards the global optimum.

The original exploration mechanism in CGO is encapsulated by (9), which generates new seeds based entirely on random values uniformly distributed within the problem's defined boundaries (LB and UB). While this ensures a broad and non-discriminatory exploration of the search domain, it can lead to suboptimal convergence behaviors due to its indiscriminate nature. The proposed strategy introduces a combination of strategic guidance and stochastic elements by utilizing both the globally best solution and a fitness-distance balanced approach to direct the exploration process more effectively. The formulation of the new exploration equation is as follows:

$$index = fitnessDistanceBalance(Seeds, fitnessSeeds) \quad (13)$$

where $index$ is determined by the $fitnessDistanceBalance$ function, which strategically selects a seed from the Seeds array by evaluating both fitness and spatial diversity criteria represented in $fitnessSeeds$.

$$perturbation = \alpha\,(BestSeed - Seed_{index}) + \beta(UB - LB) \quad (14)$$

where $perturbation$ is calculated to introduce a guided deviation towards the globally optimal position $BestSeed$, moderated by the parameter α and a random exploratory component scaled by β that respects the upper (UB) and lower (LB) bounds of the search space.

$$Seed4 = Seed_{index} + perturbation \quad (15)$$

The above equation updates the seed at $index$ by applying the $perturbation$, thus generating a new candidate solution, $Seed4$, for further evaluation in the optimization process.

This technique retains the inherent randomness essential for a robust exploration in CGO but ameliorates it with strategic inputs based on the algorithm's performance and provides a comprehension of the search landscape. This method is designed to dynamically balance between exploring uncharted territories and exploiting promising solutions, thus optimizing the performance of CGO across various complex problem landscapes. Figure 1 presents a detailed flowchart that outlines the procedural steps of the proposed algorithm.

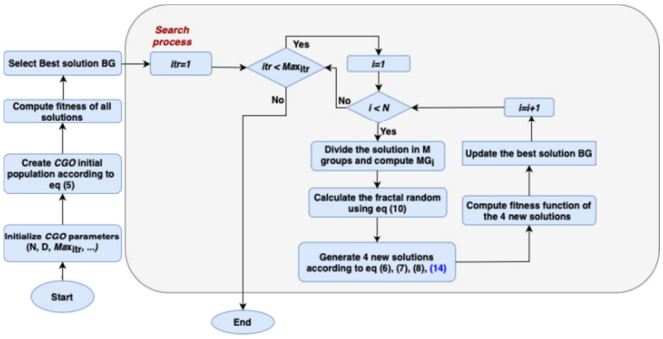

Fig. 1. Flowchart of FDB-CGO algorithm.

V. EXPERIMENTAL RESULTS

The performance of the proposed algorithm for multilevel thresholding segmentation was thoroughly evaluated. A suite of images, meticulously chosen from the USC-SIPI Image Database [57], named peppers, airplane, man, tank, and Barbara served as the dataset for this analysis. The experimental studies were executed on MATLAB R2018a, running on a workstation equipped with an AMD Ryzen 7 5800X CPU @ 3.80 GHz and 32 GB of RAM. To obtain reliable statistical insights, each algorithm was iteratively tested across 30 runs for every individual image, providing a robust sample size for analysis. This method facilitates the acquisition of a comprehensive performance dataset, allowing the calculation of mean values and standard deviations, thereby providing a substantive analysis of the algorithmic efficacy across a range of conditions and scenarios.

A. Evaluation Metrics

Two established evaluation metrics were employed to review the performance of the proposed algorithm for multilevel thresholding segmentation: Peak Signal-to-Noise Ratio (PSNR) and Structural Similarity Index (SSIM). PSNR is a reflective measure of the reconstruction quality for a segmented image, relative to its original counterpart, defined as:

$$PSNR = 10 . log_{10}\left(\frac{MAX_I^2}{MSE}\right) \quad (16)$$

where MAX_I denotes the maximum potential intensity of the image's pixel values. The Mean Squared Error (MSE), indicative of the average squared intensity differences between the segmented and original images, is given by:

$$MSE = \frac{1}{mn}\sum_{i=0}^{m-1}\sum_{j=0}^{n-1}[I(i,j) - K(i,j)]^2 \quad (17)$$

where I and K represent the original and segmented images respectively, and $m * n$ signifies the dimensions of the images. SSIM, on the other hand, quantifies the perceptual difference between two similar images. It is an advanced metric that considers changes in structural information, luminance, and contrast. The SSIM index is given by:

$$SSIM(x,y) = \frac{(2\mu_x\mu_y+c_1)(2\sigma_{x,y}+c_2)}{(\mu_x^2+\mu_y^2+c_1)(\sigma_x^2+\sigma_y^2+c_2)} \quad (18)$$

where x and y are two windowed samples of the images under comparison. The μ_x and μ_y variables represent the sample means of x and y, while σ_x^2 and σ_y^2 are the variances, and $\sigma_{x,y}$ is the covariance. The constants c_1 and c_2 serve to stabilize the fraction in situations where the denominator is small, enhancing the metric's robustness.

B. Statistical Analysis

This analysis starts with a comparison of the objective function values obtained through the implementation of different optimization algorithms, namely PSO [58], GWO [59], MFO [60], GA [61], CGO [54], and FDB-CGO, using both the Kapur and Otsu methods. The performance of these algorithms was evaluated based on their mean and standard deviation of the objective function values across various images at different threshold levels, as shown in Tables I and II. The data from the Kapur method indicate that FDB-CGO consistently outperformed the other algorithms in terms of higher mean objective function values across all images and levels. For example, in the case of the Airplane image at a threshold level of 20, FDB-CGO achieved a mean value of 66.81, significantly higher than its closest competitor, GWO, which had a mean of 50.76. This trend of superior performance of FDB-CGO is evident across the other images, particularly at higher threshold levels.

Similarly, in the evaluation using the Otsu method, FDB-CGO again showed superior performance compared to the other algorithms. For the Man image at a threshold level of 20, FDB-CGO reached a mean objective function value of 15911.09, markedly higher than the next-best score of 10559.78 by CGO. This pattern of achieving the highest mean values is consistent across all listed images and levels. Standard deviation values display the stability of the algorithms. FDB-CGO not only achieved the highest mean values, but also exhibited moderate variability, suggesting robust performance across different settings and images. While FDB-CGO tends to have higher standard deviations at higher threshold levels, these were accompanied by significantly improved mean values, indicating a trade-off between variability and performance enhancement.

1) Evaluation of Image Segmentation Algorithms Based on PSNR

Table III provides the mean PSNR values obtained from the image segmentation algorithms, applied to a set of images

using the Kapur and Otsu methods with different threshold levels. The PSNR values highlight the effectiveness of each algorithm in preserving post-segmentation image quality. Higher PSNR values indicate better preservation of image quality. In the the Kapur method, FDB-CGO frequently demonstrated competitive or superior performance, particularly at higher threshold levels. For example, in the Airplane image at level 20, FDB-CGO achieved a PSNR of 25.987, the highest among the algorithms evaluated at this level. The Otsu method showed a different trend, where FDB-CGO consistently outperformed other algorithms in various images and levels, achieving the highest PSNR values. This suggests that FDB-CGO is particularly well-tuned for the Otsu method, as noticed in the Airplane image at level 20, where it recorded 35.085 PSNR, leading the table. These results manifest that while all algorithms perform variably across different settings and images, FDB-CGO offers a more robust solution for achieving high-quality image segmentation, which is critical in applications demanding high fidelity relative to the original image.

TABLE I. COMPARISON OF OBJECTIVE FUNCTION VALUES: FDB-CGO VERSUS OTHER ALGORITHMS USING THE KAPUR METHOD

Image	Level	PSO		GWO		MFO		GA		CGO		FDB-CGO	
		mean	std	mean	std	mean	std	mean	std	mean	std	mean	std
Airplane	8	25.58	0.68	27.22	0.05	27.07	0.26	27.16	0.09	24.51	0.89	27.47	0.43
	12	33.37	0.90	37.20	0.16	35.88	0.95	36.39	0.69	32.25	1.10	41.31	0.67
	16	38.76	1.24	44.44	0.23	42.48	1.45	43.23	1.05	38.43	1.18	53.63	1.47
	20	44.30	1.27	50.76	0.40	47.77	1.69	48.57	1.49	44.32	1.56	66.81	1.38
Barbara	8	32.29	0.48	33.68	0.07	33.60	0.08	33.53	0.16	30.89	0.64	33.65	0.29
	12	44.32	0.87	47.23	0.17	46.36	0.68	46.72	0.60	42.61	1.15	48.60	1.78
	16	52.96	1.21	57.93	0.23	55.75	1.06	57.05	0.55	50.94	1.13	64.96	2.32
	20	60.62	1.20	67.17	0.25	63.92	1.46	65.99	1.26	59.29	1.27	80.35	1.64
Man	8	33.99	0.21	34.41	0.00	34.37	0.04	34.37	0.03	33.27	0.56	36.09	0.42
	12	45.99	0.84	47.85	0.05	47.38	0.38	47.66	0.19	44.80	0.64	54.02	0.71
	16	55.21	0.91	59.07	0.19	57.57	1.02	58.39	0.78	54.48	1.46	70.63	1.17
	20	63.19	1.23	68.77	0.33	65.97	1.30	67.44	1.30	63.10	1.88	87.30	1.58
Peppers	8	34.01	0.42	35.46	0.00	35.27	0.12	35.34	0.10	33.17	0.64	36.20	0.31
	12	46.23	1.02	48.75	0.06	47.94	0.58	48.25	0.55	44.83	0.90	53.62	0.99
	16	55.31	1.03	59.46	0.19	57.71	1.28	58.59	0.66	54.28	1.36	71.22	1.25
	20	62.62	1.34	68.91	0.21	65.66	1.43	67.08	0.98	62.99	1.88	87.65	1.54
Tank	8	28.16	0.87	30.47	0.18	30.38	0.18	30.36	0.23	27.30	0.72	30.75	0.23
	12	37.75	0.90	41.83	0.31	40.50	1.12	40.87	0.57	36.59	1.04	45.11	1.19
	16	45.23	1.31	50.65	0.43	47.88	1.59	48.30	1.18	44.11	1.69	58.79	2.25
	20	51.25	1.50	57.80	0.61	53.98	1.38	55.10	1.64	51.88	2.13	72.25	2.44

TABLE II. COMPARISON OF OBJECTIVE FUNCTION VALUES: FDB-CGO VERSUS OTHER ALGORITHMS USING THE OTSU METHOD

Image	Level	PSO		GWO		MFO		GA		CGO		FDB-CGO	
		mean	std	mean	std	mean	std	mean	std	mean	std	mean	std
Airplane	8	568.41	82.88	480.88	0.02	475.95	2.60	478.05	2.17	1013.76	91.43	1383.21	90.32
	12	656.59	90.65	485.08	0.25	481.43	1.55	482.33	1.59	1264.42	147.19	1933.91	134.31
	16	735.46	97.01	486.35	0.22	483.56	1.43	484.45	0.69	1525.23	156.16	2568.63	173.59
	20	747.84	76.67	487.03	0.25	484.72	1.52	485.11	1.01	1742.54	205.92	3093.35	143.53
Barbara	8	785.47	45.29	758.02	0.01	754.37	4.36	755.39	3.44	1067.60	124.17	1425.74	63.07
	12	903.31	60.37	767.89	0.19	764.10	2.68	765.44	1.78	1258.38	176.66	2040.05	92.33
	16	995.67	52.75	772.15	0.15	768.35	1.96	770.43	1.22	1480.86	151.05	2619.88	134.69
	20	1085.70	82.83	774.20	0.15	771.00	1.82	772.56	0.82	1714.54	246.74	3162.63	176.95
Man	8	3584.72	388.37	3242.90	0.00	3236.95	7.59	3239.56	4.21	5883.82	468.60	7093.90	283.23
	12	4239.45	461.00	3271.21	0.10	3263.59	5.20	3265.10	4.15	7314.42	440.11	10107.86	334.90
	16	4427.13	445.90	3281.56	0.15	3273.99	4.41	3276.39	2.99	9055.39	591.44	12904.21	506.09
	20	5025.43	533.14	3286.37	0.16	3280.64	2.83	3282.22	1.66	10559.78	787.29	15911.09	508.58
Peppers	8	3113.47	193.71	2848.94	0.01	2840.72	6.87	2844.95	6.35	4498.58	262.09	6013.70	233.18
	12	3520.52	294.46	2878.71	0.13	2868.83	6.81	2871.54	3.91	5855.11	419.09	8644.88	262.96
	16	3877.72	294.51	2888.81	0.19	2879.45	4.39	2880.31	5.29	7000.27	531.91	11153.50	406.10
	20	4033.36	831.02	2893.54	0.33	2886.04	3.01	2886.82	3.09	7893.18	518.40	13430.44	563.89
Tank	8	601.44	42.76	568.52	0.01	561.55	5.45	564.70	3.40	1128.98	168.57	1566.81	122.03
	12	610.24	126.42	574.79	0.18	567.68	3.64	569.79	2.49	1340.44	119.59	2160.74	141.98
	16	368.84	355.96	577.20	0.32	570.78	2.76	571.93	2.57	1582.23	197.73	2763.50	177.65
	20	46.26	177.25	577.87	0.78	573.02	2.06	572.90	2.32	1874.31	290.57	3355.00	231.79

2) Evaluation of Image Segmentation Algorithms Based on SSIM Metric

Table IV provides a detailed comparison of the SSIM metric for various image segmentation algorithms applied employing the Kapur and Otsu thresholding methods. The SSIM metric was applied to evaluate the segmentation quality relative to the structural integrity of the original images. The results reveal a varying performance between algorithms and methods. In the Kapur method, FDB-CGO often achieved the highest SSIM values, preserving the image structure more

competently than other algorithms. For example, in the Airplane image at level 20, FDB-CGO scored an SSIM of 0.892, which was higher compared to PSO and GWO. In the Otsu method, FDB-CGO consistently demonstrated superior performance, particularly at higher threshold levels, showing robustness in maintaining structural integrity in various operational settings. For instance, in the Man image at level 20, FDB-CGO attained an SSIM of 0.928, closely matching the highest value of 0.934 by GA, and significantly better than CGO's 0.480. These results underscore the importance of selecting appropriate segmentation algorithms based on specific requirements for image fidelity and structural preservation, especially in applications requiring high accuracy and consistency.

TABLE III. EVALUATION BASED ON MEAN PSNR METRICS ACROSS DIFFERENT THRESHOLD LEVELS AND METHODS

Image	Level	Kapur						Otsu					
		PSO	GWO	MFO	GA	CGO	FDB-CGO	PSO	GWO	MFO	GA	CGO	FDB-CGO
Airplane	8	19.899	7.500	19.689	19.598	19.290	19.471	19.023	4.987	27.774	28.011	14.839	28.459
	12	20.431	7.858	20.284	19.888	19.198	22.009	17.928	4.876	31.156	31.230	15.668	30.566
	16	16.843	6.816	21.004	21.383	17.804	23.735	18.199	4.711	32.547	33.143	15.312	33.602
	20	14.463	6.356	22.504	24.104	17.952	25.987	17.795	4.551	34.485	34.445	15.351	35.085
Barbara	8	21.163	11.886	20.726	20.975	20.634	20.301	19.829	7.906	25.042	25.134	17.200	25.292
	12	25.670	12.078	25.056	25.403	20.691	26.853	19.071	7.402	28.574	28.849	16.706	29.068
	16	24.830	12.008	26.935	28.508	16.806	29.509	18.937	7.082	30.626	31.300	16.576	31.292
	20	19.850	11.487	29.646	29.886	16.254	30.762	18.770	7.086	32.454	33.303	16.466	33.416
Man	8	23.393	14.788	23.230	23.328	16.364	23.087	18.734	9.546	24.869	25.044	15.483	25.377
	12	26.751	14.730	26.093	26.304	16.192	26.733	18.623	9.522	27.670	27.872	14.845	28.848
	16	23.480	14.616	28.114	28.376	14.410	28.573	18.787	9.337	29.525	30.000	16.173	31.284
	20	15.906	13.495	30.276	30.003	13.190	30.357	18.514	9127	31.188	31.621	16.349	33.199
Peppers	8	22.213	11.984	21.006	21.116	15.497	21.317	17.156	8.387	24.065	24.203	12.508	24.329
	12	25.807	12.028	25.102	25.366	14.148	26.098	16.696	8.357	26.822	27.209	12.909	27.976
	16	21.736	11.019	27.730	27.772	14.726	28.406	15.814	8.384	28.668	28.847	13.360	30.409
	20	16.144	10.642	28.971	29.174	11.955	30.368	15.563	8.064	30.247	30.448	13.873	32.408
Tank	8	21.144	12.797	20.800	20.828	19.205	20.826	20.350	7.601	28.444	29.201	16.998	29.883
	12	22.292	12.704	22.389	22.887	17.441	23.911	20.276	7.086	30.235	31.137	17.323	32.519
	16	20.984	11.346	25.293	24.815	16.174	26.719	20.443	7.335	31.766	32.161	18.060	34.767
	20	18.307	10.811	26.486	26.347	13.682	28.658	20.796	7.426	32.809	32.894	17.700	35.649

TABLE IV. EVALUATION BASED ON MEAN SSIM METRICS ACROSS DIFFERENT THRESHOLD LEVELS AND METHODS

Image	Level	Kapur						Otsu					
		PSO	GWO	MFO	GA	CGO	FDB-CGO	PSO	GWO	MFO	GA	CGO	FDB-CGO
Airplane	8	0.894	0.560	0.892	0.892	0.873	0.889	0.793	0.290	0.874	0.881	0.820	0.919
	12	0.866	0.590	0.898	0.897	0.871	0.906	0.751	0.271	0.919	0.920	0.800	0.947
	16	0.710	0.489	0.902	0.904	0.827	0.903	0.765	0.244	0.936	0.944	0.808	0.961
	20	0.635	0.433	0.901	0.895	0.832	0.892	0.766	0.222	0.949	0.949	0.765	0.967
Barbara	8	0.889	0.765	0.887	0.888	0.878	0.882	0.848	0.443	0.897	0.897	0.818	0.898
	12	0.920	0.775	0.916	0.918	0.843	0.923	0.837	0.368	0.922	0.920	0.816	0.909
	16	0.905	0.772	0.930	0.934	0.748	0.939	0.835	0.329	0.930	0.933	0.816	0.938
	20	0.787	0.714	0.942	0.942	0.743	0.947	0.812	0.321	0.940	0.947	0.815	0.956
Man	8	0.709	0.617	0.713	0.714	0.491	0.697	0.575	0.280	0.781	0.785	0.451	0.777
	12	0.809	0.629	0.819	0.802	0.476	0.806	0.579	0.281	0.868	0.872	0.429	0.852
	16	0.708	0.607	0.873	0.854	0.388	0.847	0.589	0.259	0.903	0.911	0.476	0.899
	20	0.471	0.509	0.913	0.893	0.341	0.881	0.569	0.241	0.928	0.934	0.480	0.928
Peppers	8	0.701	0.608	0.683	0.681	0.509	0.683	0.572	0.357	0.741	0.738	0.388	0.737
	12	0.787	0.615	0.794	0.793	0.453	0.792	0.551	0.342	0.817	0.829	0.401	0.832
	16	0.676	0.508	0.852	0.848	0.469	0.844	0.518	0.351	0.862	0.866	0.423	0.883
	20	0.484	0.474	0.879	0.878	0.354	0.885	0.510	0.304	0.893	0.896	0.445	0.917
Tank	8	0.777	0.550	0.772	0.773	0.717	0.769	0.648	0.222	0.866	0.885	0.627	0.904
	12	0.776	0.547	0.796	0.803	0.632	0.812	0.638	0.157	0.903	0.916	0.623	0.946
	16	0.719	0.468	0.828	0.820	0.577	0.832	0.640	0.177	0.925	0.932	0.625	0.962
	20	0.635	0.430	0.828	0.836	0.443	0.863	0.648	0.200	0.941	0.937	0.611	0.966

VI. CONCLUSION

This study introduced a novel approach to image processing, leveraging the innovative application of multilevel thresholding for image segmentation. This research stands out by incorporating the FDB mechanism within the CGO algorithm to address critical inefficiencies noted in previous methods. Traditional thresholding and basic metaheuristic techniques often suffer from premature convergence and need more robustness to handle complex images in diverse real-world settings. This analysis highlighted a significant gap in the ability of existing methods to balance the exploration and exploitation phases necessary for optimal segmentation. The proposed FDB-CGO algorithm demonstrated superior performance over the existing algorithms, validated through extensive experiments on benchmark datasets. The proposed algorithm had improved segmentation accuracy and reduced

computational demands, making it practical for real-time image processing applications. The results underlined the potential to integrate advanced optimization techniques with chaos theory to refine the robustness and effectiveness of image segmentation processes. Future research could refine and expand the proposed strategies for a broader application in image-based tasks. Exploring alternative combinations of metaheuristic algorithms may yield valuable insights. Advances in computational technology offer opportunities to develop more sophisticated models capable of handling larger datasets, potentially revolutionizing automated image analysis in critical sectors, such as healthcare, environmental monitoring, and autonomous systems.

REFERENCES

[1] L. Abualigah, K. H. Almotairi, and M. A. Elaziz, "Multilevel thresholding image segmentation using meta-heuristic optimization algorithms: comparative analysis, open challenges and new trends," *Applied Intelligence*, vol. 53, no. 10, pp. 11654–11704, May 2023, https://doi.org/10.1007/s10489-022-04064-4.

[2] S. Pare, A. Kumar, G. K. Singh, and V. Bajaj, "Image Segmentation Using Multilevel Thresholding: A Research Review," *Iranian Journal of Science and Technology, Transactions of Electrical Engineering*, vol. 44, no. 1, pp. 1–29, Mar. 2020, https://doi.org/10.1007/s40998-019-00251-1.

[3] M. Nssibi, G. Manita, and O. Korbaa, "Advances in nature-inspired metaheuristic optimization for feature selection problem: A comprehensive survey," *Computer Science Review*, vol. 49, Aug. 2023, Art. no. 100559, https://doi.org/10.1016/j.cosrev.2023.100559.

[4] R. V. V. Krishna and S. S. Kumar, "Hybridizing Differential Evolution with a Genetic Algorithm for Color Image Segmentation," *Engineering, Technology & Applied Science Research*, vol. 6, no. 5, pp. 1182–1186, Oct. 2016, https://doi.org/10.48084/etasr.799.

[5] M. Amiriebrahimabadi, Z. Rouhi, and N. Mansouri, "A Comprehensive Survey of Multi-Level Thresholding Segmentation Methods for Image Processing," *Archives of Computational Methods in Engineering*, Mar. 2024, https://doi.org/10.1007/s11831-024-10093-8.

[6] M. H. Horng, "Multilevel thresholding selection based on the artificial bee colony algorithm for image segmentation," *Expert Systems with Applications*, vol. 38, no. 11, pp. 13785–13791, Oct. 2011, https://doi.org/10.1016/j.eswa.2011.04.180.

[7] A. K. Bhandari, A. Kumar, and G. K. Singh, "Modified artificial bee colony based computationally efficient multilevel thresholding for satellite image segmentation using Kapur's, Otsu and Tsallis functions," *Expert Systems with Applications*, vol. 42, no. 3, pp. 1573–1601, Feb. 2015, https://doi.org/10.1016/j.eswa.2014.09.049.

[8] S. Zhang, W. Jiang, and S. Satoh, "Multilevel Thresholding Color Image Segmentation Using a Modified Artificial Bee Colony Algorithm," *IEICE Transactions on Information and Systems*, vol. E101-D, no. 8, pp. 2064–2071, Aug. 2018.

[9] P. Upadhyay and J. K. Chhabra, "Multilevel thresholding based image segmentation using new multistage hybrid optimization algorithm," *Journal of Ambient Intelligence and Humanized Computing*, vol. 12, no. 1, pp. 1081–1098, Jan. 2021, https://doi.org/10.1007/s12652-020-02143-3.

[10] P. D. Sathya and R. Kayalvizhi, "Modified bacterial foraging algorithm based multilevel thresholding for image segmentation," *Engineering Applications of Artificial Intelligence*, vol. 24, no. 4, pp. 595–615, Jun. 2011, https://doi.org/10.1016/j.engappai.2010.12.001.

[11] Y. Liu, K. Hu, Y. Zhu, and H. Chen, "Color image segmentation using multilevel thresholding-cooperative bacterial foraging algorithm," in *2015 IEEE International Conference on Cyber Technology in Automation, Control, and Intelligent Systems (CYBER)*, Shenyang, China, Jun. 2015, pp. 181–185, https://doi.org/10.1109/CYBER.2015.7287931.

[12] Y. Zhou, L. Li, and M. Ma, "A Novel Hybrid Bat Algorithm for the Multilevel Thresholding Medical Image Segmentation," *Journal of Medical Imaging and Health Informatics*, vol. 5, no. 8, pp. 1742–1746, Dec. 2015, https://doi.org/10.1166/jmihi.2015.1638.

[13] A. K. Bhandari, V. K. Singh, A. Kumar, and G. K. Singh, "Cuckoo search algorithm and wind driven optimization based study of satellite image segmentation for multilevel thresholding using Kapur's entropy," *Expert Systems with Applications*, vol. 41, no. 7, pp. 3538–3560, Jun. 2014, https://doi.org/10.1016/j.eswa.2013.10.059.

[14] J. Rahaman and M. Sing, "An efficient multilevel thresholding based satellite image segmentation approach using a new adaptive cuckoo search algorithm," *Expert Systems with Applications*, vol. 174, Jul. 2021, Art. no. 114633, https://doi.org/10.1016/j.eswa.2021.114633.

[15] A. M. Hemeida, R. Mansour, and M. E. Hussein, "Multilevel Thresholding for Image Segmentation Using an Improved Electromagnetism Optimization Algorithm," *International Journal of Interactive Multimedia and Artificial Intelligence*, vol. 5, no. 4, pp. 102–112, 2019.

[16] S. Song, H. Jia, and J. Ma, "A Chaotic Electromagnetic Field Optimization Algorithm Based on Fuzzy Entropy for Multilevel Thresholding Color Image Segmentation," *Entropy*, vol. 21, no. 4, 2019, https://doi.org/10.3390/e21040398.

[17] M. Maitra and A. Chatterjee, "A hybrid cooperative–comprehensive learning based PSO algorithm for image segmentation using multilevel thresholding," *Expert Systems with Applications*, vol. 34, no. 2, pp. 1341–1350, Feb. 2008, https://doi.org/10.1016/j.eswa.2007.01.002.

[18] Y. Huang and S. Wang, "Multilevel Thresholding Methods for Image Segmentation with Otsu Based on QPSO," in *2008 Congress on Image and Signal Processing*, Sanya, China, Feb. 2008, vol. 3, pp. 701–705, https://doi.org/10.1109/CISP.2008.76.

[19] H. Gao, W. Xu, J. Sun, and Y. Tang, "Multilevel Thresholding for Image Segmentation Through an Improved Quantum-Behaved Particle Swarm Algorithm," *IEEE Transactions on Instrumentation and Measurement*, vol. 59, no. 4, pp. 934–946, Oct. 2009, https://doi.org/10.1109/TIM.2009.2030931.

[20] L. Djerou, N. Khelil, H. E. Dehimi, and M. Batouche, "Automatic Multilevel Thresholding Using Binary Particle Swarm Optimization for Image Segmentation," in *2009 International Conference of Soft Computing and Pattern Recognition*, Malacca, Malaysia, Dec. 2009, pp. 66–71, https://doi.org/10.1109/SoCPaR.2009.25.

[21] P. D. Sathya and R. Kayalvizhi, "Development of a new optimal multilevel thresholding using improved particle swarm optimization algorithm for image segmentation," *International journal of electronics engineering*, vol. 2, no. 1, pp. 63–67, 2010.

[22] D. Yazdani, A. Arabshahi, A. Sepas-Moghaddam, and M. M. Dehshibi, "A multilevel thresholding method for image segmentation using a novel hybrid intelligent approach," in *2012 12th International Conference on Hybrid Intelligent Systems (HIS)*, Pune, India, Sep. 2012, pp. 137–142, https://doi.org/10.1109/HIS.2012.6421323.

[23] N. Apoorva, D. Ramesh, K. Manikantan, and S. Ramachandran, "Optimal multilevel thresholding based on Tsallis entropy using Fibonacci Particle Swarm Optimization for improved Image Segmentation," in *2012 International Conference on Communication, Information & Computing Technology (ICCICT)*, Mumbai, India, Oct. 2012, pp. 1–6, https://doi.org/10.1109/ICCICT.2012.6398162.

[24] A. Alva, R. S. Akash, and K. Manikantan, "Optimal multilevel thresholding based on Tsallis entropy and half-life constant PSO for improved image segmentation," in *2015 IEEE UP Section Conference on Electrical Computer and Electronics (UPCON)*, Allahabad, India, Dec. 2015, pp. 1–6, https://doi.org/10.1109/UPCON.2015.7456685.

[25] Z. Yang and A. Wu, "A non-revisiting quantum-behaved particle swarm optimization based multilevel thresholding for image segmentation," *Neural Computing and Applications*, vol. 32, no. 16, pp. 12011–12031, Aug. 2020, https://doi.org/10.1007/s00521-019-04210-z.

[26] L. Britto, L. Pacífico, and T. Ludermir, "A Multilevel Thresholding Approach Based on Improved Particle Swarm Optimization for Color Image Segmentation," in *Encontro Nacional de Inteligência Artificial e Computacional (ENIAC)*, Oct. 2020, pp. 306–317, https://doi.org/10.5753/eniac.2020.12138.

[27] K. Hammouche, M. Diaf, and P. Siarry, "A multilevel automatic thresholding method based on a genetic algorithm for a fast image segmentation," *Computer Vision and Image Understanding*, vol. 109, no. 2, pp. 163–175, Feb. 2008, https://doi.org/10.1016/j.cviu.2007.09.001.

[28] R. Kumar, T. Parashar, and G. Verma, "A multilevel automatic thresholding for image segmentation using genetic algorithm and dwt," *International Journal of Electronics and Computer Science Engineering*, vol. 1, no. 1, pp. 153–160, 2013.

[29] E. A. Baniani and A. Chalechale, "A new multilevel thresholding method using hybrid pso and genetic algorithm for image segmentation," *International Journal of Advanced Studies in Computers, Science and Engineering*, vol. 2, no. 2, pp. 18–24, 2013.

[30] S. Patra, R. Gautam, and A. Singla, "A novel context sensitive multilevel thresholding for image segmentation," *Applied Soft Computing*, vol. 23, pp. 122–127, Oct. 2014, https://doi.org/10.1016/j.asoc.2014.06.016.

[31] J. Zhang, H. Li, Z. Tang, Q. Lu, X. Zheng, and J. Zhou, "An Improved Quantum-Inspired Genetic Algorithm for Image Multilevel Thresholding Segmentation," *Mathematical Problems in Engineering*, vol. 2014, Apr. 2014, Art. no. e295402, https://doi.org/10.1155/2014/295402.

[32] H. Shah-Hosseini, "Multilevel Thresholding for Image Segmentation using the Galaxy-based Search Algorithm," *International Journal of Intelligent Systems and Applications*, vol. 5, no. 11, pp. 19–33, Oct. 2013, https://doi.org/10.5815/ijisa.2013.11.03.

[33] M. Tuba and I. Brajevic, "Modified seeker optimization algorithm for image segmentation by multilevel thresholding," *International Journal of Mathematical Models and Methods in Applied Sciences*, vol. 7, no. 4, pp. 370–378, 2013.

[34] O. Banimelhem, M. Mowafi, and O. Alzoubi, "Multilevel thresholding image segmentation using memetic algorithm," in *2015 6th International Conference on Information and Communication Systems (ICICS)*, Amman, Jordan, Apr. 2015, pp. 119–123, https://doi.org/10.1109/IACS.2015.7103213.

[35] Y. Han, W. Chen, A. A. Heidari, and H. Chen, "Multi-verse Optimizer with Rosenbrock and Diffusion Mechanisms for Multilevel Threshold Image Segmentation from COVID-19 Chest X-Ray Images," *Journal of Bionic Engineering*, vol. 20, no. 3, pp. 1198–1262, May 2023, https://doi.org/10.1007/s42235-022-00295-w.

[36] A. K. M. Khairuzzaman and S. Chaudhury, "Multilevel thresholding using grey wolf optimizer for image segmentation," *Expert Systems with Applications*, vol. 86, pp. 64–76, Nov. 2017, https://doi.org/10.1016/j.eswa.2017.04.029.

[37] M. Karakoyun, N. A. Baykan, and M. Hacibeyoglu, "Multi-Level Thresholding for Image Segmentation With Swarm Optimization Algorithms," *International Research Journal of Electronics and Computer Engineering*, vol. 3, no. 3, Sep. 2017, https://doi.org/10.24178/irjece.2017.3.3.01.

[38] P. Kandhway and A. K. Bhandari, "A Water Cycle Algorithm-Based Multilevel Thresholding System for Color Image Segmentation Using Masi Entropy," *Circuits, Systems, and Signal Processing*, vol. 38, no. 7, pp. 3058–3106, Jul. 2019, https://doi.org/10.1007/s00034-018-0993-3.

[39] H. Liang, H. Jia, Z. Xing, J. Ma, and X. Peng, "Modified Grasshopper Algorithm-Based Multilevel Thresholding for Color Image Segmentation," *IEEE Access*, vol. 7, pp. 11258–11295, 2019, https://doi.org/10.1109/ACCESS.2019.2891673.

[40] X. Bao, H. Jia, and C. Lang, "A Novel Hybrid Harris Hawks Optimization for Color Image Multilevel Thresholding Segmentation," *IEEE Access*, vol. 7, pp. 76529–76546, 2019, https://doi.org/10.1109/ACCESS.2019.2921545.

[41] S. K. Wang, H. M. Jia, and X. X. Peng, "Modified salp swarm algorithm based multilevel thresholding for color image segmentation," *Mathematical Biosciences and Engineering (MBE)*, vol. 17, no. 1, pp. 700–724, Oct. 2019, https://doi.org/10.3934/mbe.2020036.

[42] M. Ahmadi, K. Kazemi, A. Aarabi, T. Niknam, and M. S. Helfroush, "Image segmentation using multilevel thresholding based on modified bird mating optimization," *Multimedia Tools and Applications*, vol. 78, no. 16, pp. 23003–23027, Aug. 2019, https://doi.org/10.1007/s11042-019-7515-6.

[43] Z. Xing and H. Jia, "Modified thermal exchange optimization based multilevel thresholding for color image segmentation," *Multimedia Tools and Applications*, vol. 79, no. 1, pp. 1137–1168, Jan. 2020, https://doi.org/10.1007/s11042-019-08229-1.

[44] R. Kalyani, P. D. Sathya, and V. P. Sakthivel, "Trading strategies for image segmentation using multilevel thresholding aided with minimum cross entropy," *Engineering Science and Technology, an International Journal*, vol. 23, no. 6, pp. 1327–1341, Dec. 2020, https://doi.org/10.1016/j.jestch.2020.07.007.

[45] H. Li, G. Zheng, K. Sun, Z. Jiang, Y. Li, and H. Jia, "A Logistic Chaotic Barnacles Mating Optimizer With Masi Entropy for Color Image Multilevel Thresholding Segmentation," *IEEE Access*, vol. 8, pp. 213130–213153, 2020, https://doi.org/10.1109/ACCESS.2020.3040177.

[46] M. Abd Elaziz, N. Nabil, R. Moghdani, A. A. Ewees, E. Cuevas, and S. Lu, "Multilevel thresholding image segmentation based on improved volleyball premier league algorithm using whale optimization algorithm," *Multimedia Tools and Applications*, vol. 80, no. 8, pp. 12435–12468, Mar. 2021, https://doi.org/10.1007/s11042-020-10313-w.

[47] Z. Yan, J. Zhang, and J. Tang, "Modified water wave optimization algorithm for underwater multilevel thresholding image segmentation," *Multimedia Tools and Applications*, vol. 79, no. 43, pp. 32415–32448, Nov. 2020, https://doi.org/10.1007/s11042-020-09664-1.

[48] E. H. Houssein, B. E. Helmy, D. Oliva, A. A. Elngar, and H. Shaban, "A novel Black Widow Optimization algorithm for multilevel thresholding image segmentation," *Expert Systems with Applications*, vol. 167, Apr. 2021, Art. no. 114159, https://doi.org/10.1016/j.eswa.2020.114159.

[49] S. K. Dinkar, K. Deep, S. Mirjalili, and S. Thapliyal, "Opposition-based Laplacian Equilibrium Optimizer with application in Image Segmentation using Multilevel Thresholding," *Expert Systems with Applications*, vol. 174, Jul. 2021, Art. no. 114766, https://doi.org/10.1016/j.eswa.2021.114766.

[50] S. Wang, K. Sun, W. Zhang, and H. Jia, "Multilevel thresholding using a modified ant lion optimizer with opposition-based learning for color image segmentation," *Mathematical Biosciences and Engineering*, vol. 18, no. 4, pp. 3092–3143, Apr. 2021, https://doi.org/10.3934/mbe.2021155.

[51] S. Mahajan, N. Mittal, and A. K. Pandit, "Image segmentation using multilevel thresholding based on type II fuzzy entropy and marine predators algorithm," *Multimedia Tools and Applications*, vol. 80, no. 13, pp. 19335–19359, May 2021, https://doi.org/10.1007/s11042-021-10641-5.

[52] J. N. Kapur, P. K. Sahoo, and A. K. C. Wong, "A new method for gray-level picture thresholding using the entropy of the histogram," *Computer Vision, Graphics, and Image Processing*, vol. 29, no. 3, pp. 273–285, Mar. 1985, https://doi.org/10.1016/0734-189X(85)90125-2.

[53] N. Otsu, "A Tlreshold Selection Method from Gray-Level Histograms," *Automatica*, vol. 11, pp. 285–296, 1975.

[54] S. Talatahari and M. Azizi, "Chaos Game Optimization: a novel metaheuristic algorithm," *Artificial Intelligence Review*, vol. 54, no. 2, pp. 917–1004, Feb. 2021, https://doi.org/10.1007/s10462-020-09867-w.

[55] H. T. Kahraman, S. Aras, and E. Gedikli, "Fitness-distance balance (FDB): A new selection method for meta-heuristic search algorithms," *Knowledge-Based Systems*, vol. 190, Feb. 2020, Art. no. 105169, https://doi.org/10.1016/j.knosys.2019.105169.

[56] M. W. Ouertani, G. Manita, and O. Korbaa, "Automatic Data Clustering Using Hybrid Chaos Game Optimization with Particle Swarm Optimization Algorithm.," *Procedia Computer Science*, vol. 207, pp. 2677–2687, Jan. 2022, https://doi.org/10.1016/j.procs.2022.09.326.

[57] "The USC-SIPI Image Database." University of Southern California, [Online]. Available: https://sipi.usc.edu/database/.

[58] J. Kennedy and R. Eberhart, "Particle swarm optimization," in *Proceedings of ICNN'95 - International Conference on Neural Networks*, Perth, Australia, Nov. 1995, vol. 4, pp. 1942–1948 vol.4, https://doi.org/10.1109/ICNN.1995.488968.

[59] S. Mirjalili, S. M. Mirjalili, and A. Lewis, "Grey Wolf Optimizer," *Advances in Engineering Software*, vol. 69, pp. 46–61, Mar. 2014, https://doi.org/10.1016/j.advengsoft.2013.12.007.

[60] S. Mirjalili, "Moth-flame optimization algorithm: A novel nature-inspired heuristic paradigm," *Knowledge-Based Systems*, vol. 89, pp. 228–249, Nov. 2015, https://doi.org/10.1016/j.knosys.2015.07.006.

[61] J. H. Holland, Adaptation in Natural and Artificial Systems: An Introductory Analysis with Applications to Biology, Control, and Artificial Intelligence. MIT Press, 1992.